



## **OPTIMISED ARRAY DESIGN FOR MICROTREMOR ARRAY STUDIES APPLIED TO SITE CLASSIFICATION; COMPARISON OF RESULTS WITH SCPT LOGS.**

**Authors: Michael W. ASTEN<sup>1</sup>, Trevor DHU<sup>2</sup> and Nelson LAM<sup>3</sup>**

### **SUMMARY**

The microtremor method (MTM) using spatial autocorrelation (SPAC) processing is a useful tool for gaining thickness and shear wave velocity (SWV) of sediments. These parameters are essential for site response modeling and regolith classification for earthquake hazard and risk assessments. Complications arise if the wave field is strongly directional (ie. insufficiently averaged in azimuth) or contains multiple Rayleigh modes. Theoretical studies compare the use of triangular, hexagonal and semi-circular arrays and show how the latter is preferable in the presence of strongly directional seismic noise, while the hexagonal array is superior in maximising the range of detectable wavelengths. Both hexagonal and semi-circular arrays can identify multiple-mode wave propagation.

Observed coherency-frequency curves are inverted in coherency space (without the intermediate step of obtaining a dispersion curve from field data) to yield a profile of SWV and layer thicknesses to depths up to one hundred metres. The MTM using SPAC has achieved a precision of  $\pm 10\%$  or better in the Vs30 zone of unconsolidated but moderately homogeneous sediments. The results show a good to strong correlation with seismic cone penetrometer tests (SCPTs) from Perth (Western Australia). Moreover, the microtremor data has an additional advantage of being capable of non-invasively detecting the base of sediments where the SCPT method fails in coarse gravels.

MTM combined with SPAC has the potential to provide SWV profiles of soils and near-surface basement rocks, suitable for input into a site response model.

### **INTRODUCTION**

The background to the microtremor method (MTM) used for estimating shear-wave velocities (SWVs) has been reviewed by many authors (eg. Tokimatsu [1]; Asten [2]; Okada [3]; Asten, [4]). Microtremors are the background movement of the earth attributable to non-seismic sources. In the frequency band of interest in this study (1 to 30 Hz), sources are principally cultural noise such as vehicle traffic and industrial machinery. For studies in metropolitan areas, the MTM is especially useful as the seismic noise

---

<sup>1</sup> Centre for Environmental and Geotechnical Applications of Surface Waves (CEGAS), School of Geosciences, Monash University, Melbourne Australia. Email: masten@mail.earth.monash.edu.au

<sup>2</sup> Geoscience Australia, Canberra Australia. Email: Trevor.Dhu@ga.gov.au

<sup>3</sup> CEGAS, Dept. of Civil Engineering, Univ. of Melbourne, Australia Email: n.lam@civag.unimelb.edu.au

which degrades active seismic methods (such as seismic reflection and refraction surveys) provides a plentiful source of energy for passive seismic methods.

Microtremor seismic energy propagates primarily as surface waves, with the majority of the energy in the fundamental mode. Vertical-component geophones will detect only Rayleigh waves, while horizontal-component instruments detect both Rayleigh and Love modes. See Asten [5, 2] Asten and Dhu [6] and Okada [3] for reviews of studies of the modes of microtremors. Microtremor studies using three-component arrays of geophones have been reported by Chouet [7] and Okada [3] but the use of vertical-component SPAC processing remains the most common approach.

The fundamental Rayleigh mode generally dominates high-frequency microtremor energy, and the basic spectral ratio method of site classification, as well as more sophisticated interpretation tools such as the spatial autocorrelation or spatially averaged coherency (SPAC) method, assume energy is confined to this single mode. However, this restriction is not always the case, and higher modes can be identified, both in the spectra shown in this paper, and in measured propagation velocities (eg Asten [2]; Bodin [8]; Asten [9]). Higher modes of surface-wave propagation have the potential to influence both measured microtremor spectra and measured propagation velocities, both of which affect the interpretation of regolith thickness and geotechnical properties.

The majority of studies using microtremor wave-fields can be placed into two groups, specifically: single station spectral methods, and array studies where the propagation velocity is sought. In the first group, the use of single-station horizontal/vertical spectral ratios (HVSR) of seismic microtremors is now a standard tool for calculating natural site period. This natural period can then be used in regolith site classification for earthquake hazard and risk studies (Nakamura [10]; Field and Jacobs [11]; Lermo and Chavez-Garcia [12]; Lachet and Bard [13]; Ibs von Seht and Wohlenberg [14]). Plots of spectral ratio against period may show multiple peaks which may be loosely described as harmonics of shear-wave resonances (Bodin *et al*[8]), but can be more rigorously analysed in terms of higher-mode Rayleigh-wave propagation (Asten [9]).

In the second group of studies, array methods are used to measure the phase velocities of microtremor energy. The most successful results from array studies of high-frequency microtremors ( $> 1\text{Hz}$ ) have been achieved using the SPAC method first described by Aki [15]. The strength of SPAC techniques is that they are effective in yielding wave scalar velocity when the wave field is multi-directional or omnidirectional. In contrast, beam-forming methods as used by eg. Capon [16], Liu *et al* [17], and Satoh *et al* [18], lose resolution when multiple sources are present, even when waves are restricted to a single mode.

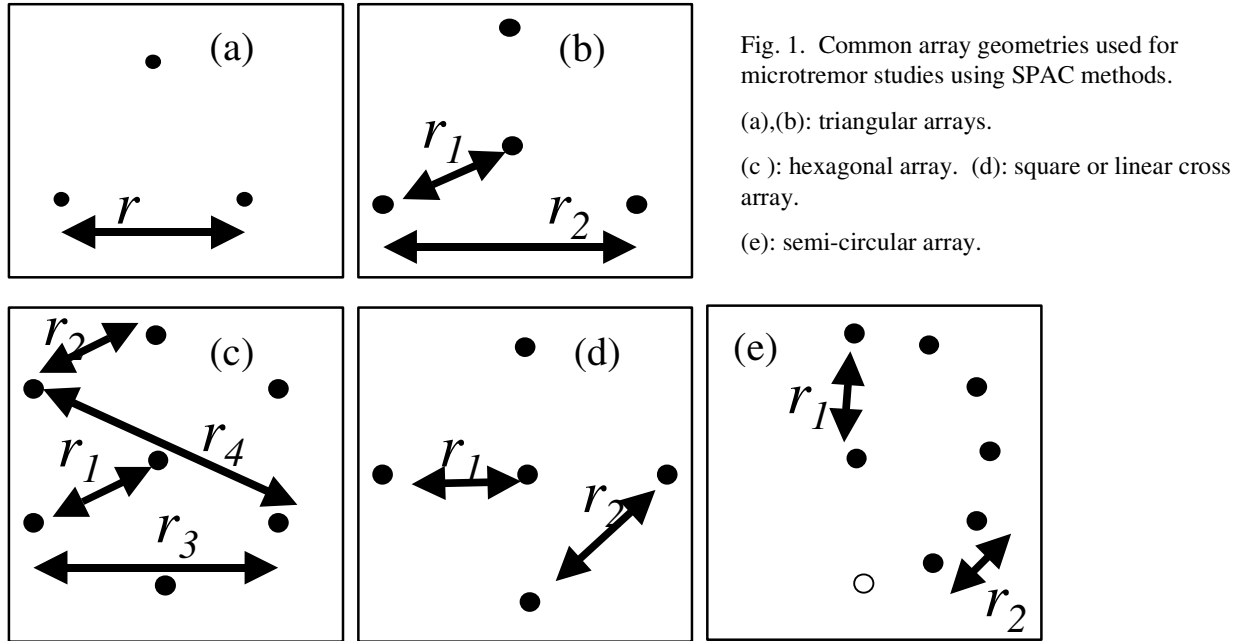
In this paper we study five array types in order to develop criteria for assessing the effectiveness of the spatial averaging process, and to recognise features of field data which indicate when assumptions of spatial averaging have been violated with adverse effects on accuracy of phase velocity estimates. We then apply the SPAC method to three samples of field data where known geology allows a assessment of the accuracy of a novel inversion method for SPAC data, performed in coherency space rather than velocity space. Finally we consider the implications of this tool for earthquake risk and site response studies.

## ARRAY GEOMETRIES

Critical to the success of the SPAC method is the effectiveness of spatial averaging achieved by the combination of array geometry and distribution of sources. In this paper we review some properties of five array types in order to develop criteria for adequacy of the spatial averaging process, and to recognise

features of field data which indicate when assumptions of spatial averaging have been violated with adverse effects on accuracy of phase velocity estimates.

The classic array shapes reported in literature are triangular three or four-station arrays shown in Figure 1 (a-b). Asten [5, 2], Asten *et al* [20] and Asten *et al* [21] use a seven-station hexagonal array (Figure 1c) in order to improve spatial averaging and provide measurements over multiple inter-station separations. More dense arrays of up to 36 stations in a semi-circular geometry have been used by Chouet *et al* [7] (and references therein), for the study of surface-wave propagation near volcanoes. However, this sophistication of design is rarely possible in microtremor surveys intended to cover multiple sites. Ohori *et al* [19] used a linear cross array which can be approximated for the purpose of this study as a five-station square array (Figure 1d) or as a right-angled triangle. This paper also considers a semi-circular array of seven stations (Figure 1e) representing a simplification of that described by Chouet *et al* [7].



## MODELLING SPAC

The process of modelling SPAC for an azimuthal distribution of noise-free plane waves, as observed by a set of geophone pairs distributed in azimuth, may be expressed as a summation of complex coherencies  $c(f)$  of amplitude unity, and phase given by

$$c(f) = \exp \{ i r k \cos(\theta - \phi) \},$$

where  $r$  is the displacement of one geophone relative to a reference geophone, at azimuthal angle  $\theta$ ,  $k$  is the spatial wavenumber at frequency  $f$ , and  $\phi$  is the azimuth of propagation of the plane wave across the array.

In the ideal case of a single plane wave observed by an infinity of geophones placed around a circle centred on a single reference geophone, the summation is expressed as an integration which yields a purely real SPAC, given by Okada [3], equ. 3.72, as

$$\frac{1}{2\pi} \int_0^{2\pi} \exp\{irk \cos(\theta - \phi)\} d\theta = J_0(rk) \quad - (1)$$

where  $J_0$  is the Bessel function of the first kind of zero order with the variable  $rk$ . The same result will be obtained for omni-directional plane waves (an infinity of azimuths) observed by a single pair of geophones (ie integrate over  $\phi$  with  $\theta$  fixed).

In this study we investigate the quality of this approximation when the plane wave sources are restricted to a range of azimuths  $\Delta$  (where  $\Delta < 90^\circ$ ), and a finite number of  $n$  geophones equi-spaced around a circle or semi-circle. For simplicity the azimuthal range is approximated in this study by a finite set of propagation directions at intervals of  $1^\circ$  over the range  $\Delta$ . We make the strict assumption that wave energy at any frequency propagates at a single scalar velocity (commonly the fundamental Rayleigh mode for vertical-component microtremor energy). The left-hand side of equ (1) thus becomes a double summation over a finite number of plane waves, and  $n$  geophone pairs. The averaged coherency is in general a complex number, hence we compare both the real and imaginary parts of the summation with the theoretical ideal of the function  $J_0$ . We also assume for the purpose of simplicity in modelling that the scalar wave velocity is constant with respect to frequency; this assumption is not true in practice, but it does not affect the SPAC method or the conclusions of this study since SPAC averaging is applied to each frequency-wavenumber independently.

Figure 2 shows modelled SPAC wave-number spectra for the case of a square cross array, where the incident wave-field is narrow in azimuthal spread ( $\Delta = 5^\circ$ ) from four different azimuths ( $0^\circ$  to  $30^\circ$ ).

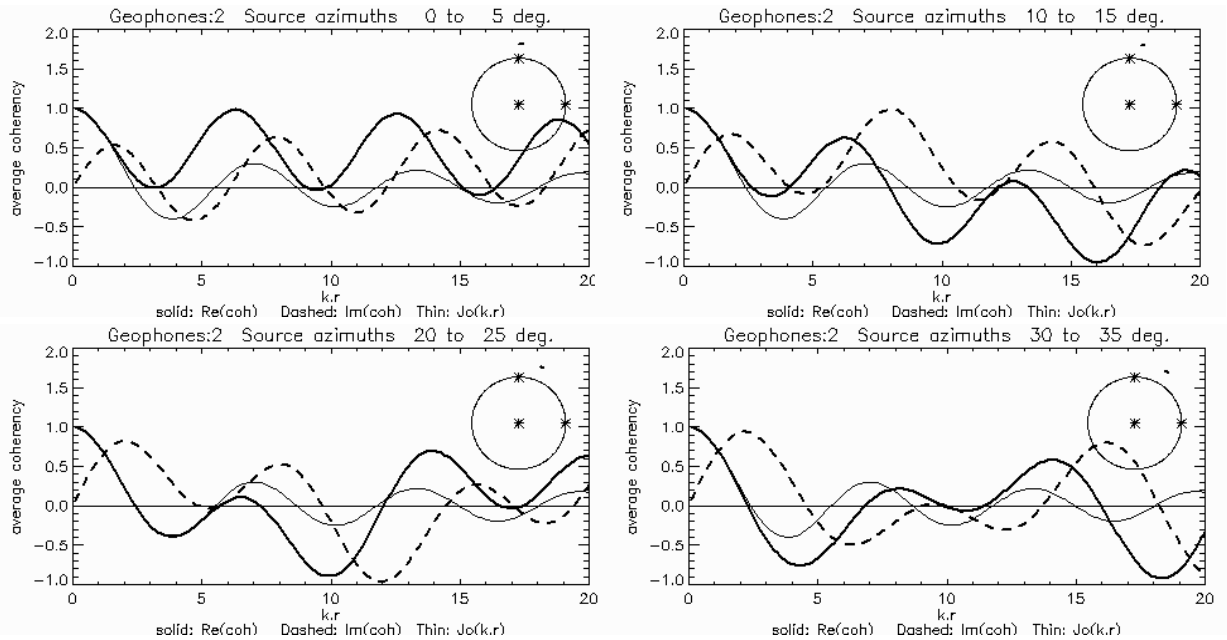


Fig. 2. Modelled SPAC for  $n=2$ ,  $\Delta=5^\circ$ , for four different dominant directions of wave propagation. The solid line is *Real* ( $c(f)$ ), dashed line is *Im* ( $c(f)$ ), and the thin solid line is theoretical  $J_0(kr)$ . At the top right of each plot is a diagram of the array geometry (centre plus two geophones only in this case) together with an arc depicting the range of wave azimuths summed in the model. The modelled SPAC curve overlays the plot of the theoretical  $J_0(kr)$  curve for  $kr \leq 2.5$ .

Spatial (azimuthal) averaging for this geometry is provided by just two directions  $90^\circ$  apart. It is evident that the modelled SPAC curve approximates the ideal ( $J_0$ ) curve only to the first cross-over ( $kr \leq 2.5$ ).

Figure 3 shows modelled SPAC wave-number spectra for the case of a triangular array, where the incident wave-field is  $\Delta = 5^\circ$ , and spatial (azimuthal) averaging is provided by three directions  $60^\circ$  apart. It is evident that the modelled SPAC curve approximates the ideal ( $J_0$ ) curve only to the first minimum ( $kr \leq 3.5$ ). The model SPAC curve for the first secondary maximum and higher frequencies is highly dependent on, and unstable with respect to, the source azimuth of this narrow spread of wave energy. This array geometry is the most common geometry used in reported MTM studies. It is implicit in the use of such arrays that the limited spatial averaging provided by the placement of geophones is compensated by greater averaging provided by a larger azimuthal spread of energy sources. Asten [22] shows that complete averaging is only achieved with the triangular array when the source spread equals the geophone angular spread ( $\Delta = 60^\circ$ ). However there are field situations where the spread of energy sources does not approach the omni-directional ideal due to the location of major roads with, for example, undulations or intersections which produce a dominant source azimuth relative to the array, regardless of the length of data acquisition.

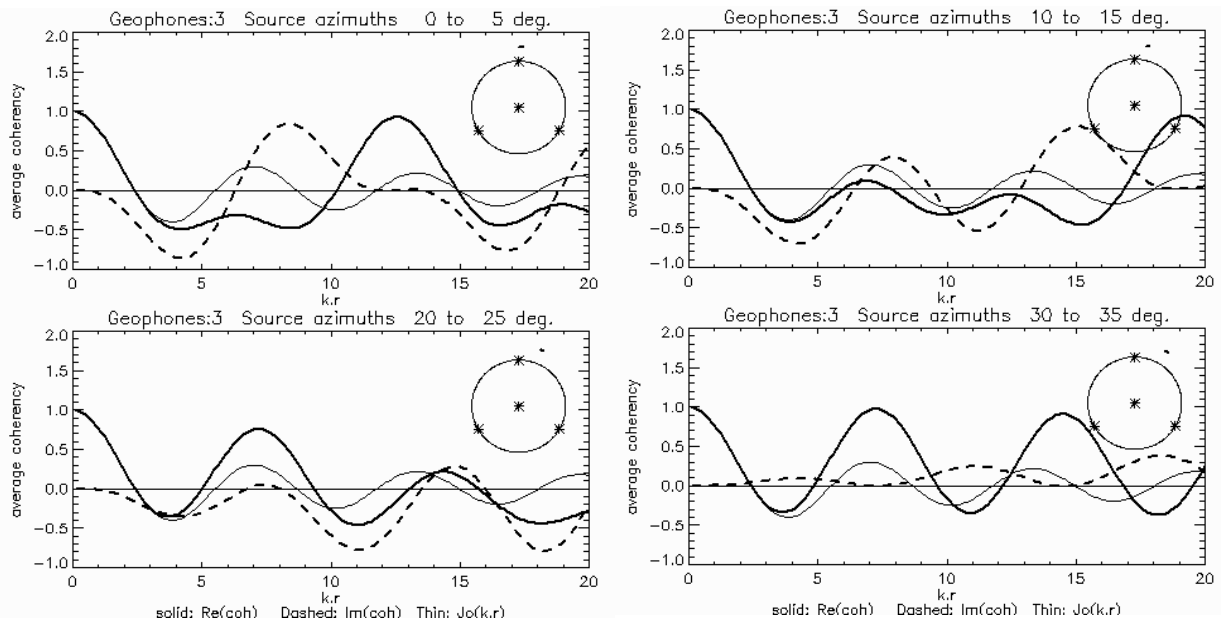


Fig. 3. As for Fig. 2, but with  $n=3$ , modelling triangular array geometries. The modelled SPAC curve overlays the plot of the theoretical  $J_0(kr)$  curve for  $kr \leq 3.5$ .

Figure 4 shows modelled SPAC spectra for the case of a semi-circular array, where the incident wave-field is  $\Delta = 5^\circ$ , and spatial (azimuthal) averaging is provided by six directions  $30^\circ$  apart. It is evident that the modelled SPAC curve is much improved, and approximates the ideal ( $J_0$ ) curve to at least the second minimum ( $kr \leq 8$ ). It may be concluded that where dominant seismic noise sources exist at fixed locations, significant improvements in the SPAC technique are possible using a semi-circular rather than triangle-based geometry.

### The imaginary component of SPAC as a quality control tool

Coherency is a complex number, but the imaginary component is rarely reported in SPAC observations. This is probably due to the fact that it is zero for all wavenumbers in the ideal case of complete spatial averaging. Study of Figures 2 to 4 shows that the spectral curves of the imaginary component of SPAC have a predictable character analogous to a quadrature waveform relative to the real component (the analogy becomes weaker as the azimuthal spread of the sources increases).

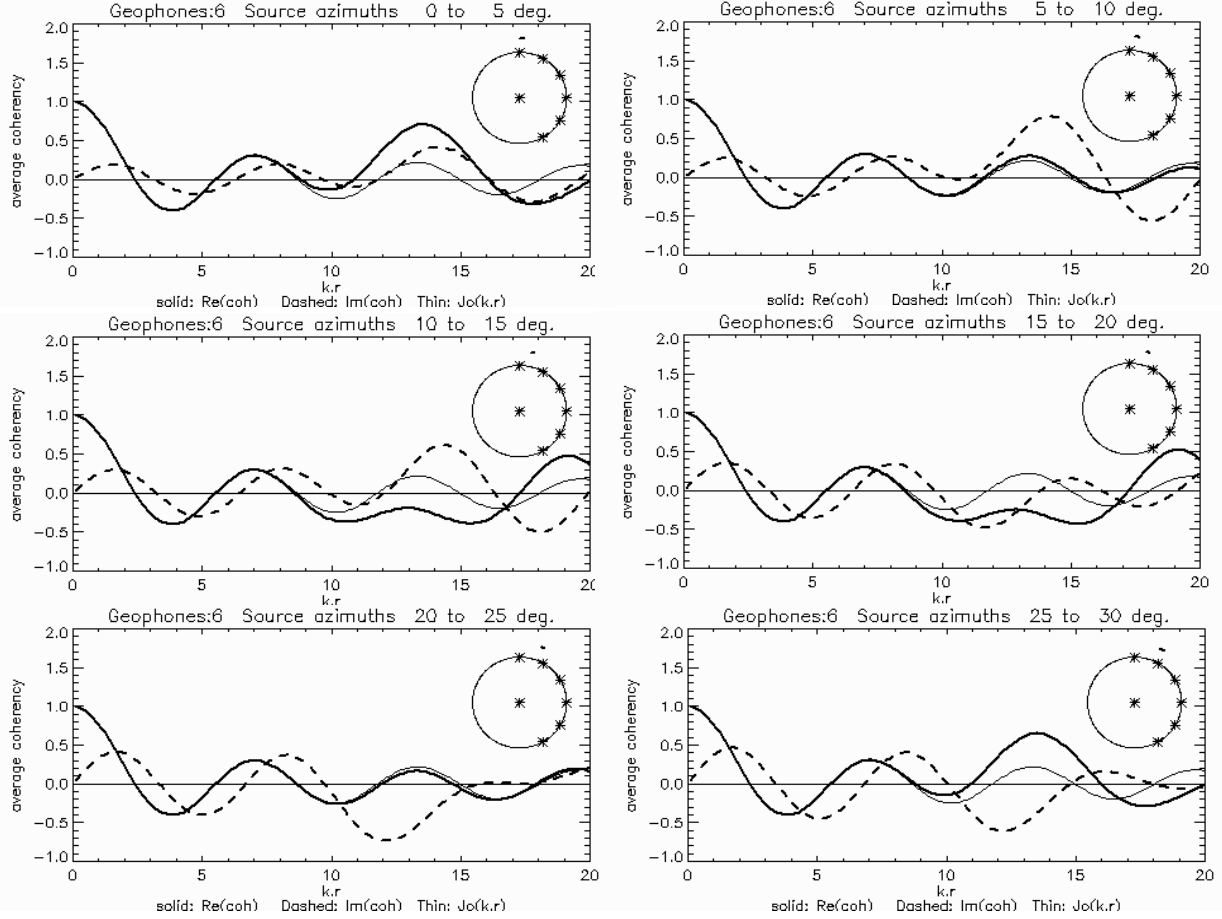


Fig. 4. As for Fig. 2, but with  $n=6$ , modelling a semi-circular array geometry. The modelled SPAC curve overlays the plot of the theoretical  $Jo(kr)$  curve for  $kr \leq 8$ .

Figure 5 shows modelled SPAC wave-number spectra for the case of a hexagonal array as used in Asten [2] and Asten *et al* [20, 21]. As with Figure 3, the incident wave-field is  $\Delta=5^\circ$ , and spatial (azimuthal) averaging is provided by three directions  $60^\circ$  apart. The real part of the SPAC is unchanged from the upper

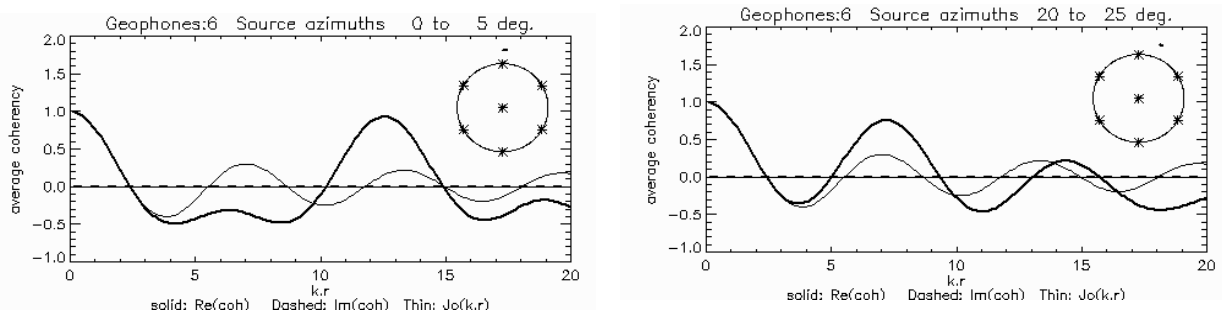


Fig. 5. As for Fig. 3, but with  $n=6$ , distributed around the full circle as a hexagonal array. The modelled SPAC curve (thick black line) is identical to the corresponding models of Figure 3.

However the imaginary part of the SPAC spectrum (dashed line) is everywhere zero.

two plots from Figure 3, since the sampling of azimuths provided by the hexagon (a set of triangles) is unchanged. However the imaginary part of the SPAC is everywhere zero. It is easy to show that this latter

theoretical result will apply for any circular array having an even number of geophones distributed around the circumference.

We can conclude that plotting the imaginary component of SPAC field data provides two additional measures of data quality:

- a) In the case of the triangular or semi-circular array, irregular maxima or minima in SPAC spectra will occur in both real and imaginary spectra if azimuthal sampling and averaging provided by the array is incomplete as a result of the presence of dominant sources.
- b) In the case of a hexagonal array (or larger and even number of stations), the imaginary part of the SPAC spectrum will be ideally zero *irrespective* of the presence of dominant sources, and in such a case the imaginary curve becomes a direct measure of statistical noise in the coherency estimates generated from field data. Figure 7 shows an example of this on field data.

## FITTING MODEL AND FIELD DATA

The classical approach to interpretation of SPAC data is to undertake a two-stage process where the SPAC spectrum is first inverted to velocities by numerical solution to equ (1). These velocities form a phase-velocity dispersion curve, usually considered to be the dispersion curve for fundamental-mode Rayleigh waves. The second stage of the process is to fit the phase velocities to a model dispersion curve computed for a layered earth, either by curve matching or numerical inversion. Following the procedure used by Asten *et al* [20, 21] and Roberts and Asten [23] which is similar to that demonstrated by Chouet *et al* [7], we bypass the first stage and perform the fitting of model and field data in coherency space. This is found to be a more robust process and reduces biases produced by poor velocity estimates. Model coherencies are easily computed as a forward modelling exercise using a surface-wave layered earth modelling program such as that by Herrmann [24] followed by computation of model SPAC values by application of equ (1).

### Field Data

Geoscience Australia acquired five MTM datasets as part of its earthquake risk assessment of Perth (Western Australia) (Figure 6). Samples from Sites 2 and 4 are considered within this paper.. In each example, field data was acquired with two circular arrays of radii 25 m and 50 m, although only one array is discussed for each of the examples reported here. The sensors used were 1 Hz Mark L4C-3D geophones. For each array, the central geophone was connected to record all three components, so as to allow comparison of HSVR data with array velocity data. Geophones on the circumference recorded the vertical component only. The modelling for Site 4 was carried out with the aid of shear-wave velocities from SCPT. However, the SCPT data for Site 2 was withheld during the first phase of the interpretation process, thus allowing for a blind study of the interpretation process.

#### *Site 4 - Warwick*

Figure 7 presents observed and modelled coherencies for an array at Site 4, Warwick. As shown by The hexagonal array allows four independent estimates of SPAC averaging in azimuth over the four radial separations ( $r_1=r$ ,  $r_2=r$ ,  $r_3=1.7r$  and  $r_4=2r$ ) shown in Figure 1c (Asten [5, 2]). SPAC spectra for three of these station separations (48, 83, 96 m) are shown in Figure 7. This site has an SCPT measurement within 50 m of the array, and a drill-hole 1 km south of the site. Figure 8 shows a SWV profile model constructed from the SCPT and drill-hole data, together with a modified result obtained by iterative fitting to gain the coherency match shown in Figure 7. The two SWV models are a close match except for layer 3 where the MTM resolves a SWV which is 20% lower than that derived from the SCPT data. The match is still a close one for the purposes of computing site response, and the difference may be explained by the

difference between the localised measurement of a SCPT procedure vs the averaging over a 100 m diameter “foot-print” of the seismic array.



Fig. 6. Location of a profile of five microtremor array sites, northern suburbs of Perth (W.A.).

#### *Site 2 – Crimea Ten Park*

Figures 10 and 11 present SWV vs. depth profiles and observed SPAC coherencies at Site 2, Crimea Ten Park. The data from this site was initially modelled using depths obtained from a drill-hole, and velocities based on assumed SWV of the given sand/clay content. The drill-hole section is notable for containing a thickness of 23 m of clays underneath 53 m of mainly sands, and also for having a shallow thin layer of calcareous cemented sand or “coffee rock” at a depth of 2 m. These features raise the question whether the MTM can identify an inversion in the velocity-depth profile. Results of iterative fitting of the SPAC coherency data in Figure 11 shows that the velocity inversion associated with the thick basal clay layer is resolved. However, the modelling shows no indication of the existence of the thin band of near-surface coffee-rock.

Figure 12 shows a new starting model for Site 2 based on the SCPT data, (supplied after completion of the previous interpretation). The SCPT penetrated only to a depth of 18.8 m, presumably halted by coarse sands. The velocity model yielded by SCPT alone is plotted in Figure 12 (red line, partially



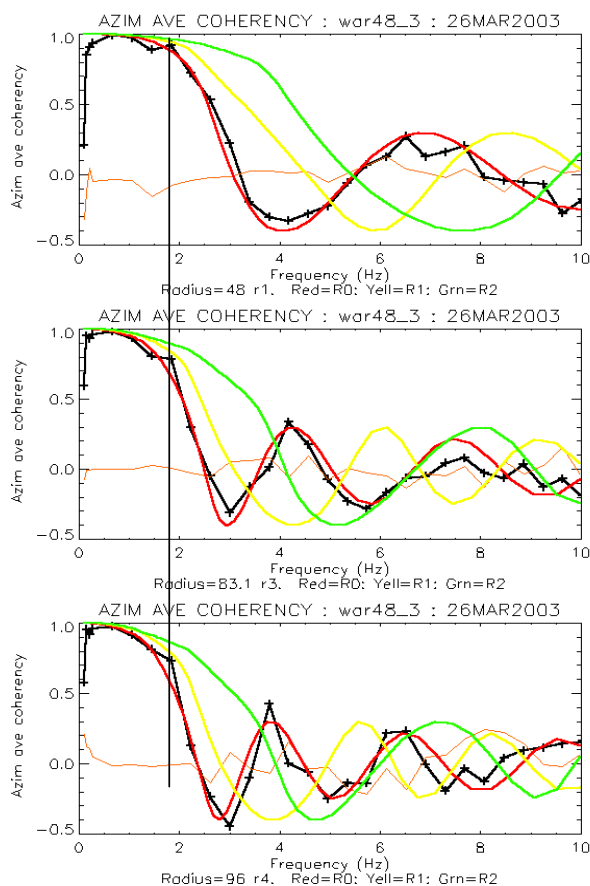


Fig. 7. Site 4: Observed coherencies (black) for station separations 48, 83, 96 m, and modelled coherencies (red) for the “best fit” model from Fig. 4. The fit for the fundamental Rayleigh mode R0 (red line) is good over the range 0.5 to 10 Hz. The points at 1.8 Hz fit R1 higher-mode energy (yellow line). Fitting of model and field data in coherency space is performed simultaneously for the three station separations.

The brown curve is the imaginary part of the coherency spectrum, and serves as an indicator of statistical noise in the field data.

Fig. 9. RIGHT: Site 4: Warwick Open Space. TOP: Observed H/V spectrum.

BOTTOM: H/V particle motion ellipticity for three modes, computed for the best-fit layered-earth model of Fig. 8. Red line: particle motion for fundamental Rayleigh mode. Yellow: 1st higher mode. Green: 2nd higher mode.

The marker at period 0.55 sec (frequency 1.8 Hz) corresponds to an H/V minimum in the first higher mode.

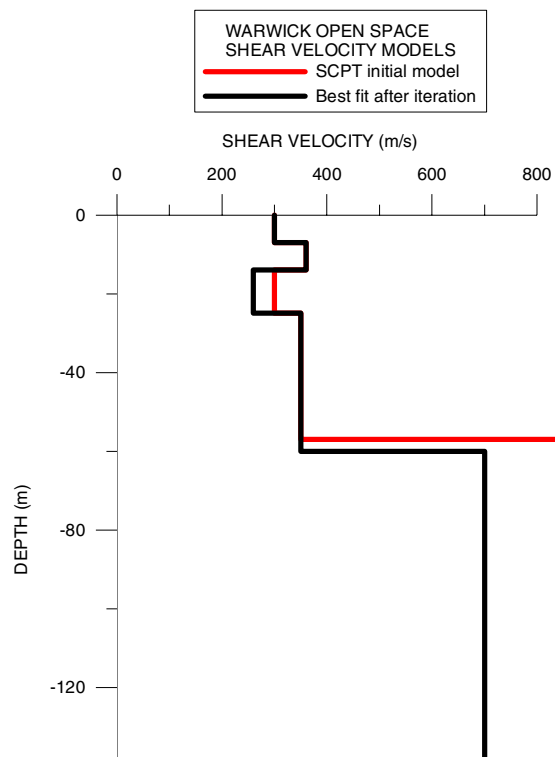
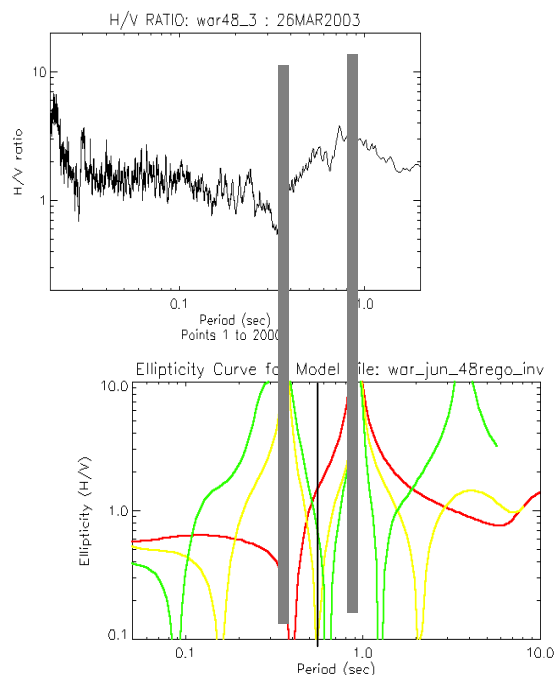


Fig. 8. ABOVE: Red line is the initial model based on SCPT and a drill-hole. Black line is the best fit after model iteration. Velocities for the top 3 layers are resolved to  $\pm 10\%$  or better. Layer 3 is the only significant discrepancy between SCPT data and microtremor-derived shear velocity.



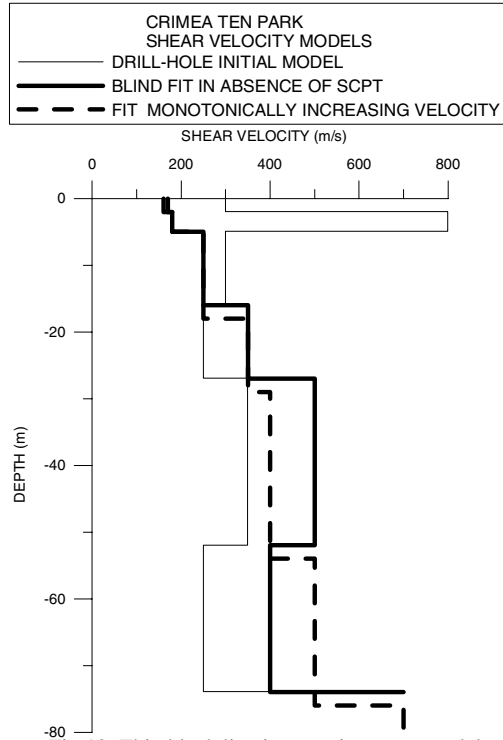


Fig.10. Thin black line is a starting model constructed from borehole data without knowledge of SCPT data. Heavy black is the best fit layered earth after iteration. Dashed line is best fit using a monotonically increasing Vs profile.

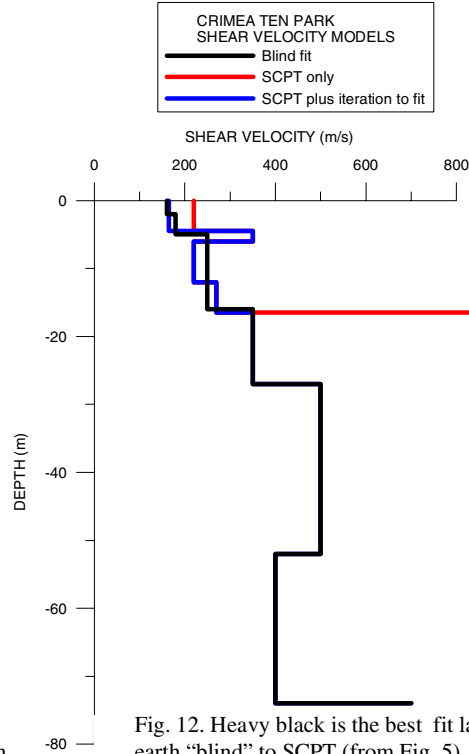


Fig. 12. Heavy black is the best fit layered earth "blind" to SCPT (from Fig. 5). Red line is a model derived from SCPT data only (apparent basement at 18.5 m). Blue line is SCPT model combined with drill-hole data to 75 m, after iteration to fit SPAC data.

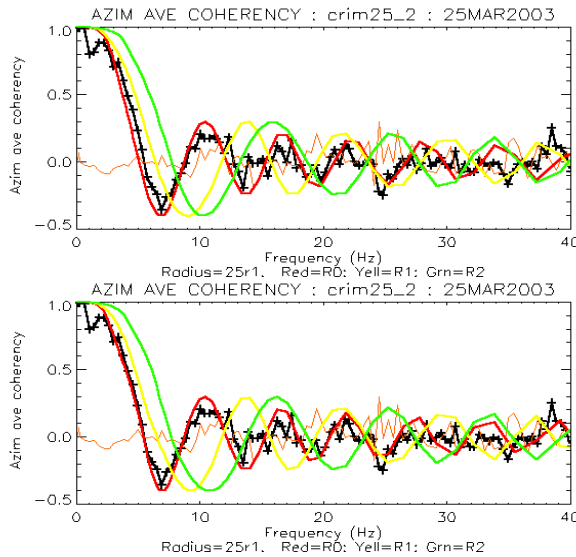


Fig.11. Site 2 Crimea Ten Park : Observed (black) and modelled (red) coherencies for station separation 25 m.

TOP: best fit using a monotonically increasing shear velocity with depth. Red line is the modelled fundamental mode. Yellow and green lines are modelled higher modes, included only for reference.

BOTTOM: best fit using the model with the low velocity layer shown in Fig. 5. In the second model, the fit is improved for frequencies 2-7 Hz. In each case, fitting of field and model coherencies was performed simultaneously for station separations of 25, 43.3 and 50 m, but only the 25 m data are shown here.

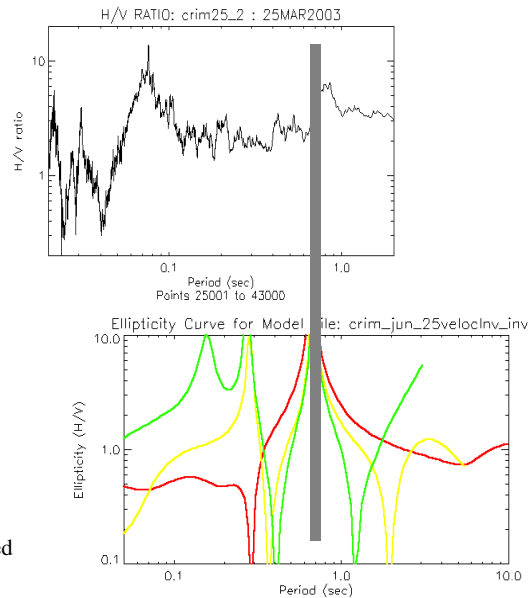


Fig. 13. Site 2 Crimea Ten Park. TOP: Observed H/V spectrum.

BOTTOM: H/V particle motion ellipticity for two modes, for the "blind fit" layered-earth model of Fig. 10. Red line: particle motion for fundamental Rayleigh mode. Yellow: 1st higher mode. Green: 2nd higher mode.

obscured by over-printing of the blue curve) and gives a very poor fit of modelled and observed SPAC data (not shown). This result is in part expected due to the erroneously-shallow basement yielded by the SCPT. However, when the SCPT velocities to 18 m are combined with layer thickness to 75 m yielded by the drill-hole data, the resultant velocity model (Figure 12, blue curve) is very close to that derived without benefit of the SCPT data. For depths 4 to 18 m the SCPT shear velocities correspond exactly with SPAC-derived velocities, while at shallow depths 0 to 5 m, the former are about 25% higher than velocities required for fitting the SPAC data. A discrepancy at such shallow depths may be explicable due to the difficulty of identifying shear arrivals in SCPT measurements at very shallow depths. The existence of the low-velocity layer corresponding to the basal clay (below the depth of SCPT measurements) is confirmed in the SPAC data. An important discrepancy between SCPT and SPAC results relevant to geotechnical engineering applications is that the SPAC data does *not* resolve any indication of the thin harder layer (presumably coffee rock) which was detected by the SCPT at a depth of 5 to 6 m (Figure 12).

Figure 13 shows the observed and modelled HVSR ratios for the site. The important resonance peak in observed data is at period 0.8 sec, but is surprisingly weak. Coupled with the difficulty in obtaining SCPT data to the base of sands and clays, this weakness provides an example where HVSR plus SCPT may produce an incomplete classification of site conditions, whereas the MTM array data is able to explicitly resolve a SWV profile.

## RECOGNITION OF MULTIPLE MODES

Asten [2] showed an example whereby the redundancy provided by three simultaneous SPAC spectra over three station separations allows recognition of multiple modes of Rayleigh-wave propagation in the microtremor field. The process of recognition of multiple modes is easier in coherency space when the majority of the spectrum fits the fundamental-mode model data, but occasional field-coherency data points show a consistent match to a higher mode model coherency. Figure 7 shows such an example at 1.8 Hz; the higher coherency is consistent across all three station separations. Note that for comparison SPAC data at different station separations to be valid, the raw data must be acquired simultaneously, ie with the one array.

Figure 9 shows the HVSR for Site 4, together with modelled HVSR computed using the velocity model derived for the site. The observed principal peak and principal trough at periods 0.9 and 0.36 sec respectively align with similar features in modelled particle-motion profiles, typical of the condition of soft sediments overlying a sharp velocity boundary (Stephenson [25]). It is interesting to note that the frequency at which the higher mode energy is noted on the SPAC spectra (1.8 Hz) also happens to be a frequency of HVSR minimum in the modelled first higher mode. Since HVSR minima relate to P-wave resonances (just as HVSR maxima relate to S-wave resonances) we have a possible explanation for the occurrence of this higher-mode feature. It is possible that re-examination of historic SPAC data in this way may show some apparently “poorly fitting data points” to be valid data from another propagation mode.

The ability of the process of curve matching in coherency space using simultaneous fitting of data from multiple station separations, to identify multiple modes, prompts us to adopt the term “multi-mode SPAC” or MMSPAC for this variant of the MTM array processing methodology.

## EXAMPLE OF SPAC DATA WITH A SEMI-CIRCULAR ARRAY

Modelling studies shown in Figure 4 suggest that the semi-circular array will have advantages when the microtremor wave-field contains dominant sources such as a nearby highway. Figure 14 shows two separate data samples from a site near Botany Bay, Sydney, where about 34 m of Quaternary sands overlie

competent Triassic sandstone. The data was recorded at separate times (each data length 200 sec). The field data SPAC spectra are each composed of an average over six radially-separated pairs of geophones, over the same radius of 48 m. The difference is that the second sample has finer sampling in azimuth and should be less prone to distortion of the SPAC spectra by dominant sources from the adjacent highway.

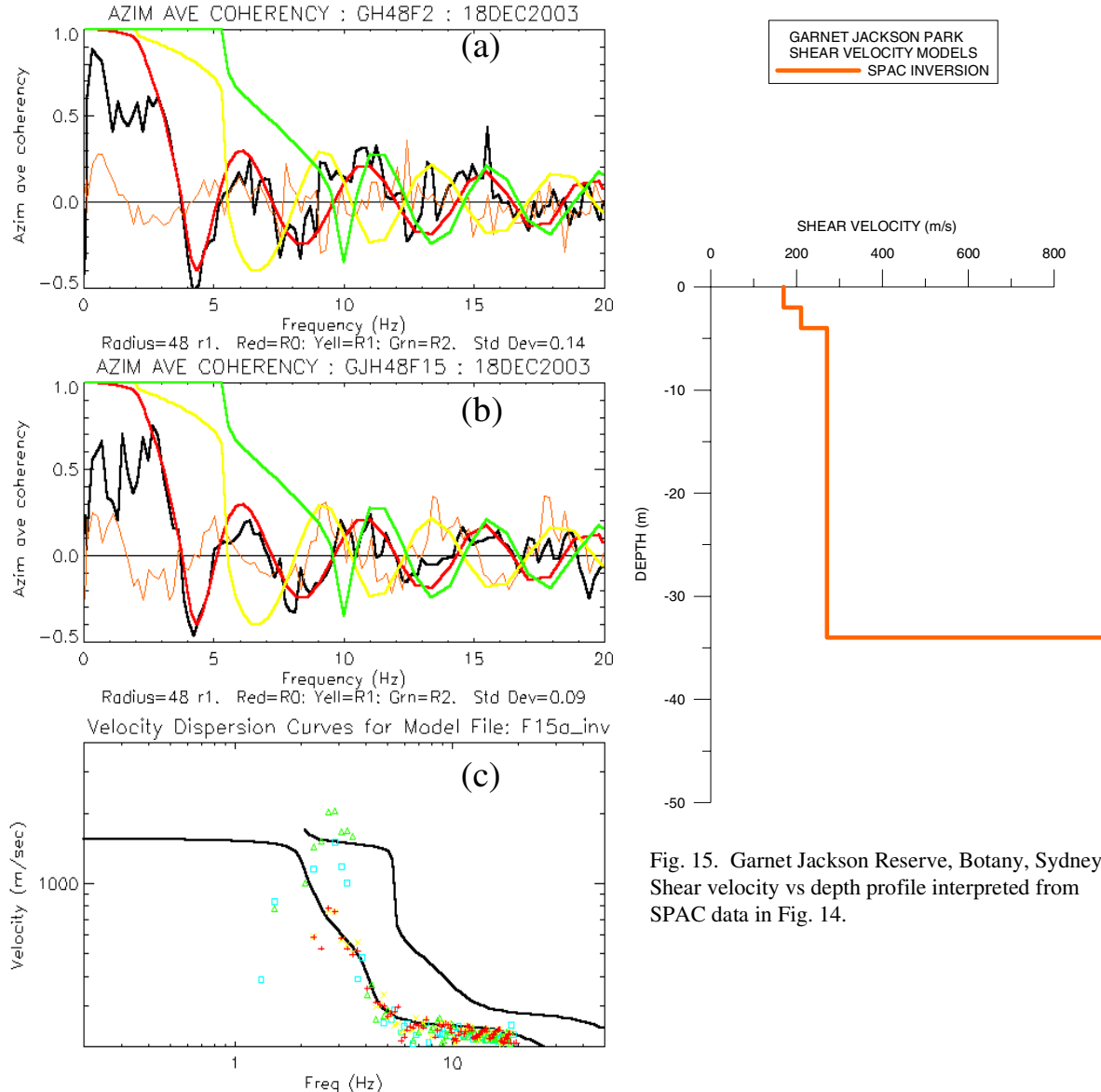


Fig. 15. Garnet Jackson Reserve, Botany, Sydney. Shear velocity vs depth profile interpreted from SPAC data in Fig. 14.

Fig. 14. Garnet Jackson Reserve, Botany, Sydney. (a): Field (black) and modelled (red) SPAC for a hexagonal array, radius 48 m. The standard deviation of the fit to the fundamental-mode model SPAC is 0.14, for data in the interval 2.5 to 17 Hz.

(b): Field and modelled SPAC for a semi-circular array, radius 48 m. The standard deviation of the fit to the fundamental-mode model SPAC is 0.09, for data in the interval 2.5 to 17 Hz.

(c) Phase velocities computed from field coherencies in (b), plotted on modelled dispersion curves of the first two Rayleigh modes.

SPAC data for frequencies below 2.5 Hz are poor, for reasons unknown at this time. For frequencies above 2.5 Hz, the SPAC spectrum for the semi-circular array is visually noticeably superior; an

observation supported by comparison of additional data files (not included here). As a measure of the quality of fit, the standard deviation of the error between field and model SPAC spectra, for the frequency band 2.5 to 17 Hz, has been computed; the standard deviation for the semi-circular array is 0.09 which is significantly superior to the value of 0.14 obtained with the hexagonal array. The disadvantage of the semi-circular array is that it provides SPAC estimates over only two station separations, compared with three for the hexagonal array (Figure 1c and 1e).

## **CONCLUSIONS AND FUTURE APPLICATION TO EARTHQUAKE HAZARD SITE AMPLIFICATION STUDIES**

The application of the MMSPAC method to data from Perth has demonstrated that SWV profiles derived by iterative fitting of observed and modeled coherencies have comparable accuracy to SCPT measurements. This has been demonstrated both by direct comparison and by a blind study where SCPT data has been disclosed after completion of a SWV interpretation. The MTM has the notable advantages over SCPT measurements that it uses purely passive seismic sources, is non-invasive, and yields shear-wave velocity estimates at depths below the limits imposed by coarse sands or gravels on SCPT measurements. In locations where dominant wave-field directions violate the assumptions inherent in the SPAC method and degrade data, modelling suggests, and field examples support, the conclusion that the use of a semi-circular array can improve the effectiveness of the MTM.

The ability of the MTM to derive a SWV profile extends to cases where the HVSr method fails to produce significant spectral peaks. The MTM therefore provides greater certainty in site classification than the HVSr method in cases where shear-wave velocity contrasts are low or gradational.

The MTM combined with the SPAC method of array processing, as described in this paper, enables the SWV profile of the earth crust to be measured directly in an inexpensive and non-intrusive manner. Good resolution of the SWV can be obtained down to a depth at least equal to the diameter of the array of geophones which is chosen to suit the nature of the regolith. Examples in this paper use radii of 25 to 48 m, but in thicker zones of Quaternary soils, radii up to 300 m and 500 m have been used successfully (Asten [26]; Okada [3]) with depth penetrations of up to six or ten times the array aperture (Apostolidis *et al* [27]; Okada [3] respectively).

SPAC processing also has the potential to be used to obtain SWV information in bedrock for studying crustal modification properties. Obtaining the same SWV information by conventional methods, such as the instrumentation of deep drill holes, is arguably expensive, time-consuming and intrusive to the environment. Through seismological modelling and stochastic simulations SPAC is potentially a significant contributor to the studies of regional attenuation properties. This is briefly described in the following.

Regional P-wave velocity information for the entire globe is now publicly available (Global Crustal Model CRUST2.0 [28]). A model which defines the depth-dependent P-wave/S-Wave velocity ratio has been developed by Chandler *et al* [29]. Consequently, regional P-wave velocity information reported in CRUST2.0 can be translated into SWV information. However, the information contained in such regional databases lacks detail at shallow depths. With the development of SPAC, the extended regional information on SWV can now be combined with shallow SWV information (Chandler *et al*, [29]). Using a proposed curve-fitting strategy, the SWV profile measured from SPAC for the shallow depth range (<200m) is combined with a deeper, regional SWV profile. This combined SWV profile enables a broad-band crustal amplification function to be calculated, using the method proposed by Boore and Joyner [30].

In a recent modelling development, these SWV profiles have been correlated with regional parameters, namely  $Q$  and  $Kappa$ , which define the energy absorption properties of the earth's crust (Chandler *et al*, [31]). The estimation of these parameters by conventional seismological methods would require extensive monitoring of local seismic activities. The measurement of  $Kappa$ , in particular, has been difficult in regions of low-to-moderate seismic activity where strong motion data is difficult to obtain. Hence, the ability to determine  $Q$  and  $kappa$  from correlations with SWV profiles could circumvent the lack of strong motion data in regions of low-to-moderate seismicity.

One future direction of our research will be to demonstrate that seismological parameters relating to both crustal amplification and attenuation mechanisms can be confidently and quickly determined from SWV profiles estimated from SPAC processing of MTM data.. When the logistics involving the deployment of large as well as small circular arrays for temporary purposes is resolved, a representative and reliable seismological model should be obtainable from surface measurements at the locality of interest. This is clearly to be preferred over the current approach of importing "analogue" models from elsewhere, often another continent, based on *ad-hoc*, and often subjective, judgement.

Once key seismological parameters have been ascertained, artificial accelerograms that are consistent in frequency properties with the parameters can be generated by stochastic simulations (eg. using program GENQKE developed by Lam *et al* [32]). The corresponding response spectral properties can be calculated accordingly using standard tools in structural dynamics. The Component Attenuation Model (CAM) provides one platform for facilitating this transformation of seismological information into response spectrum information for engineering applications (refer reviews by Lam and Wilson [33, 34]).

The proposed joint methodology of combining SPAC with CAM has considerable potential for engineering applications worldwide, especially in low-to-moderate seismic regions where strong motion records needed for conventional modelling are often lacking. An important feature of this predictive model is the estimation of the earthquake induced displacement demand which is related directly to both structural and non-structural damage.

We plan future research along the dual paths of developing the MTM methodology to acquire SWV profiles for shallow basement as well as soils and regolith, and confirming accuracy of such SWV models by comparing modelled structural damage scenarios with actual damage scenarios observed from past earthquake events.

## ACKNOWLEDGEMENTS

Field data was acquired as part of collaborative research between Monash University and Geoscience Australia, funded jointly by Geoscience Australia, Monash University, and Flagstaff GeoConsultants. The authors thank Messrs. Trevor Jones, Andrew Jones and Terry Smith of GA for their assistance in the planning, data acquisition and interpretation of the data. The array modelling was performed under Grant #4HQGR0030 of the USGS NEHRP External Grants Program. Surface-wave forward-modelling software used in the interpretation was provided by Dr R. Herrmann.

## REFERENCES

1. Tokimatsu, K. "Geotechnical site characterization using surface waves", in *Earthquake Geotechnical Engineering*, edited by Ishihara. Rotterdam: Balkema, 1997.
2. Asten, M.W., 2001, "The Spatial Auto-Correlation Method for Phase Velocity of Microseisms – Another Method for Characterisation of Sedimentary Overburden": in *Earthquake Codes in the Real*

- World, Australian Earthquake Engineering Soc., Proceedings of the 2001 Conference, Canberra, 2001, Paper 28.
3. Okada, H. (2003) "The Microseismic Survey Method", Society of Exploration Geophysicists of Japan. Translated by Koya Suto, Geophysical Monographs Vol 12. Tulsa: Society of Exploration Geophysicists, 2003.
  4. Asten, M.W., "Historical note and preface to SEG translation of "The Microseismic Method", in H. Okada, "Microseismic Survey Method": Society of Exploration Geophysicists of Japan. Translated by Koya Suto, *Geophysical Monographs*, Vol 12. Tulsa: Society of Exploration Geophysicists, 2003.
  5. Asten M.W. "The use of microseisms in geophysical exploration": PhD Thesis, Macquarie University, 1976.
  6. Asten, M.W. and Dhu, T. "Enhanced interpretation of microtremor spectral ratios using multimode Rayleigh-wave particle-motion computations", in *Total Risk Management in the Privatised Era*, edited by M Griffith, D. Love, P McBean, A McDougall, B. Butler, Proceedings of Conference, Australian Earthquake Engineering Soc. , Adelaide, Paper 8, 2002.
  7. Chouet, B., De Luca, G., Milana, G., Dawson, P., Martini, M., and Scarpa, R. "Shallow velocity structure of Stromboli Volcano, Italy, derived from small aperture array measurements of Strombolian tremor". *Bull. Seism.Soc. Am.* 1998: Vol 88: pp. 653-666.
  8. Bodin, P., Smith, K., Horton, S., and Hwang, H., 2001. "Microtremor observations of deep sediment resonance in metropolitan Memphis, Tennessee", *Engineering Geology* 2001: 62: 159-168.
  9. Asten, M.W., 2004a, "Comment on "Microtremor observations of deep sediment resonance in metropolitan Memphis, Tennessee" by Paul Bodin, Kevin Smith, Steve Horton and Howard Hwang. *Engineering Geology* 2004: 72 (3/4): 343-349.
  10. Nakamura, Y. "A method for dynamic characteristics estimation of subsurface using microtremors on the ground surface", *Quarterly reports of the Railway Technical Research Institute Tokyo* 2001: 30: pp 25-33.
  11. Field,E.H.,and Jacobs,K.H. "A comparison and test of various site-response estimation techniques, including three that are not reference-site dependent", *Bull. Seism. Soc. Am.* 1995: 85 : pp 1127-1143.
  12. Lermo, J. and Chavez-Garcia "Are microtremors useful in site response evaluation? ", *Bull. Seism. Soc. Am.* 1994: 84: pp 1350-1364.
  13. Lachet, C. and Bard,P. "Numerical and theoretical investigations on the possibilities and limitations of Nakamura's technique", *J. Phys. Earth.* 1994: 42 : pp 377-397.
  14. Ibs-von Seht,M. and Wohlenburg,J. "Microtremor measurements used to map thickness of soft sediments", *Bull. Seism. Soc. Am.* 1999: 89: pp 250-259.
  15. Aki, K. "Space and time spectra of stationary stochastic waves, with special reference to microtremors". *Bull, Earthq. Res. Inst.* 1957: 35: pp 415-456.
  16. Capon, J. "High-resolution frequency-wavenumber spectrum analysis". *Proc. IEEE* 1969: 57: pp 1408-1418.
  17. Liu H, Boore DM, Joyner WB, Oppenheimer DH, Warrick RE, Zhang W, Hamilton JC & Brown LT. "Comparison of phase velocities from array measurements of Rayleigh waves associated with microtremor and results calculated from borehole shear-wave velocity profiles". *Bull. Seism. Soc. Am.* 2000: 90: pp 666-678.
  18. Satoh,T., Kawase,H.,Iwata,T.,Higashi,S.,Sato,T., Irikura,K.,Huand,H. "S-wave velocity structure of the Taichung basin, Taiwan", estimated from array and single-station records of microtremors, *Bull. Seism. Soc. Am.* 2001: 91: pp 1267-1282.
  19. Ohori, M., Nobata, A., and Wakamatsu, K. "A comparison of ESAC and FK methods of estimating phase velocity using arbitrarily shaped microtremor arrays". *Bull. Seism. Soc. Am.* 2002 : 92: pp. 2323-2332.
  20. Asten,M.W., Lam, N., Gibson, G. and Wilson, J. "Microtremor survey design optimised for application to site amplification and resonance modelling", in *Total Risk Management in the Privatised*

- Era, edited by M Griffith, D. Love, P McBean, A McDougall, B. Butler, Proceedings of Conference, Australian Earthquake Engineering Soc. , Adelaide, Paper 7. 2000.
21. Asten, M.W., Dhu, T., Jones, A., and Jones, T. "Comparison of shear-velocities measured from microtremor array studies and SCPT data acquired for earthquake site hazard classification in the northern suburbs of Perth W.A.", in "Earthquake Risk Mitigation", (Eds) J.L. Wilson, N.K. Lam, G. Gibson, B. Butler, Proceedings of a Conference of the Australian Earthquake Engineering Soc., Melbourne, Paper 12. 2003.
  22. Asten, M.W., (2003b) "Lessons from alternative array design used for high-frequency microtremor array studies", in "Earthquake Risk Mitigation", (Eds) J.L. Wilson, N.K. Lam, G. Gibson, B. Butler, Proceedings of a Conference of the Australian Earthquake Engineering Soc., Melbourne, Paper 14.
  23. Roberts, J., and Asten, M.W., "Resolving a velocity inversion at the geotechnical scale using the microtremor (passive seismic) survey method". Exploration Geophysics 2004: 36(1): 00-00, in press.
  24. Herrmann, R.B., "Computer programs in seismology - an overview of synthetic seismogram computation Version 3.1", Department of Earth and Planetary Sciences, St Louis Univ. 2001
  25. Stephenson, W. "Factors bounding prograde Rayleigh-wave particle motion in a soft-soil layer". Proceedings of the 2003 Pacific Conference on Earthquake Engineering, Christchurch, February 2003, Paper 56, New Zealand Soc. of Earthqu. Eng. 2003.
  26. Asten, M.W., "Method for site hazard zonation, Santa Clara valley: Thickness and shear-velocity mapping of Holocene-Pleistocene sediments by array studies of microtremors". First Annual Northern California Earthquake Hazards Workshop, January 13-14, 2004, USGS, Report, Menlo Park, 2004 in press.
  27. Apostolidis, P., Raptakis, D., Roumelioti, Z., Pitilakis, K., "Determination of S-wave velocity structure using microtremors and SPAC method applied in Thessaloniki (Greece)", Soil dynamics and earthquake engineering 2004: 24: 49-67.
  28. Global Crustal Model CRUST2.0 (2001). Institute of Geophysics and Planetary Physics, The University of California, San Diego. Website: <http://mahi.ucsd.edu/Gabi/rem.dir/crust/crust2.html>.
  29. Chandler, A.M., Lam, N.T.K. and Tsang, H.H. "Shear Wave Velocity Modelling in Bedrock for Analysis of Intraplate Seismic Hazard". Soil Dynamics and Earthquake Engineering. Submitted. 2004.
  30. Boore D.M. & Joyner W.B "Site Amplifications for Generic Rock Sites". Bulletin of the Seismological Society of America 1997: 87: 327-341.
  31. Chandler, A.M., Lam, N.T.K. and Tsang, H.H. and Sheikh, M.N. "Estimation of Near-Surface Attenuation in Bedrock for Analysis of Intraplate Seismic Hazard", International Journal of Seismology and Earthquake Engineering. Submitted. 2004.
  32. Lam N.T.K., Wilson J.L., Hutchinson G.L. "Generation of synthetic earthquake accelerograms using seismological modeling: a review". Journal of Earthquake Engineering 2000: 4(3): 321-354.
  33. Lam, N.T.K., and Wilson, J., "The Component Attenuation Model for Low and Moderate Seismic Regions", Procs. of the Sixth Pacific Conference of Earthquake Engineering, University of Canterbury, Christchurch, New Zealand, March 2003. Paper no.99. 2003
  34. Lam, N.T.K., and Wilson, J., "Displacement Modelling of Intraplate Earthquakes", International Seismology and Earthquake Technology Journal (invited paper for the special issue on Performance Based Seismic Design), 2004. Indian Institute of Technology. 2004 In press.